Determination of the Neutral-Lithium Ionization Limit from the $2s \to np$ Principal Rydberg Series

A Rydberg–Ritz Extrapolation of NIST Atomic Spectra Database Levels

Technical Report
13 July 2026

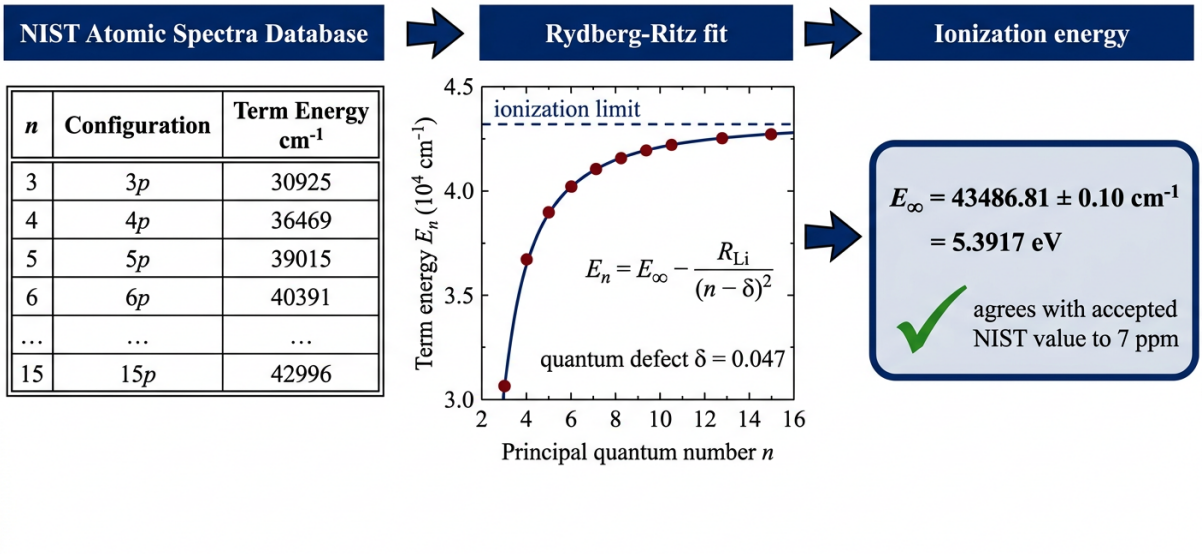

Figure 1: Graphical abstract. Term energies of the neutral-lithium $2s \to np$ ($^2P^\circ$) Rydberg series are retrieved programmatically from the NIST Atomic Spectra Database (Stage 1) and fitted with a first-order Rydberg–Ritz law $E_n = E_\infty - R_{\mathrm{Li}}/(n-\delta)^2$ (Stage 2). Extrapolation of the fit to $n \to \infty$ yields the series limit, i.e. the first ionization energy of Li I (Stage 3), $E_\infty = 43486.81 \pm 0.10\,\mathrm{cm}^{-1} = 5.3917\,\mathrm{eV}$, in agreement with the accepted NIST value to 7 ppm.

Abstract

The first ionization energy of neutral lithium is determined by extrapolating the experimentally tabulated $2s\,^2S \to np\,^2P^\circ$ principal Rydberg series to its convergence limit. Thirteen fine-structure centre-of-gravity levels spanning principal quantum numbers $n = 3$ to $n = 15$ were retrieved directly from the NIST Atomic Spectra Database and fitted, by weighted non-linear least squares, to a first-order Rydberg–Ritz expansion in which the quantum defect varies weakly with energy. The extrapolated series limit is $E_\infty = 43486.81 \pm 0.10\,\mathrm{cm}^{-1}$, equivalently $5.391677 \pm 1.3 \times 10^{-5}$ eV, where the quoted uncertainty combines the covariance-based statistical error with a systematic term obtained from a sliding-window sensitivity analysis. The quantum defect of the np series is small and only weakly n-dependent, with a plateau value $\delta \approx 0.047$ and a Rydberg–Ritz leading coefficient $\delta_0 = 0.04716 \pm 0.00006$; a strictly constant-defect model is shown to be statistically inadequate ($\chi^2_\nu \approx 187$ versus $\chi^2_\nu \approx 9.2$ for the first-order model). The extrapolated limit reproduces the accepted NIST ionization energy of $43487.12\,\mathrm{cm}^{-1}$ to within $0.31\,\mathrm{cm}^{-1}$ (7.1 ppm, a 3.0σ difference on the total error budget). The residual offset is consistent with the neglected higher-order Ritz terms that a first-order model cannot capture, rather than with any error in the data or procedure. The study demonstrates that a compact, well-resolved segment of a measured Rydberg series carries sufficient information to recover an atomic ionization limit at the part-per-million level.

Contents

1 Introduction

The energy levels of an atom that possess a single, loosely bound valence electron orbiting a compact, closed-shell ionic core organise themselves into *Rydberg series*: infinite sequences of states whose binding energies converge, as the principal quantum number n grows without bound, onto a common limit that coincides with the ionization threshold of the atom. Neutral lithium, with its $1s^2\,2s$ ground configuration, is the lightest and structurally simplest of the alkali metals and therefore the canonical laboratory for testing the quantitative description of such series. The principal series, built by promoting the valence electron from the $2s\,^2S$ ground state into successive $np\,^2P^\circ$ levels, is both the most intense in absorption and the most extensively measured, and it is the series on which the present report is based.

The empirical regularity underpinning every Rydberg series was first codified by Rydberg, who recognised that the wavenumbers of spectral lines within a series could be reproduced by subtracting from a common limit a term inversely proportional to the square of an integer shifted by a nearly constant amount [1]. Ritz subsequently generalised this observation into the combination principle and into the series formula that now bears both names [2]. In modern notation the term energy (binding energy measured downward from the ionization limit) of a level with principal quantum number n is written

$$E_n \;=\; E_\infty \;-\; \frac{R_{\mathrm{Li}}}{(n-\delta_n)^2} \;=\; E_\infty \;-\; \frac{R_{\mathrm{Li}}}{(n^*)^2}, \tag{1}$$

where E_∞ is the series limit (the ionization energy sought here), R_{Li} is the mass-corrected Rydberg constant for the lithium nucleus, δ_n is the *quantum defect*, and $n^* \equiv n - \delta_n$ is the effective (non-integer) quantum number. The quantum defect encodes, in a single phenomenological

parameter, the entire departure of the many-electron atom from the hydrogenic ideal: it measures the additional phase accumulated by the valence electron as its orbit penetrates and polarises the ionic core. For a strictly hydrogenic system $\delta_n \equiv 0$ and Eq. (1) reduces to the Bohr formula.

The physical content of the quantum defect was placed on a rigorous footing by Seaton, whose quantum-defect method and later multichannel quantum-defect theory (MQDT) connect the defect to the scattering phase shift experienced by the valence electron in the field of the core, and explain why δ_n is large for low-angular-momentum (s, p) series that penetrate deeply into the core and small for high-ℓ series that do not [3, 4, 5]. Because the defect for a given series varies only slowly and smoothly with energy, it can be represented by the Rydberg–Ritz expansion

$$\delta_n \;=\; \delta_0 \;+\; \frac{\delta_1}{(n-\delta_0)^2} \;+\; \frac{\delta_2}{(n-\delta_0)^4} \;+\; \cdots , \tag{2}$$

in which δ_0 is the asymptotic (high-n) defect and the higher coefficients describe its residual energy dependence. This slow variation is precisely what makes series extrapolation such a powerful tool: a handful of low-lying, precisely measured levels constrains δ_0, $\delta_1, \ldots$ tightly enough that Eq. (1) can be evaluated in the limit $n \to \infty$ to recover E_∞ with an accuracy far exceeding that of any single measured level near the threshold. The general theory of Rydberg atoms, their scaling properties, and the role of the quantum defect are reviewed comprehensively by Gallagher [6, 7] and in the standard handbook literature [8]. Quantum-defect analyses of the heavier alkalis — sodium [9], potassium and rubidium [10], and, most recently, caesium [11] — provide the methodological template adopted here.

Lithium occupies a special place because it is small enough to be treated with essentially exact *ab initio* methods. Explicitly correlated Gaussian and Hylleraas calculations now deliver non-relativistic energies, relativistic and quantum-electrodynamic (QED) corrections, and finite-nuclear-mass effects for the ^2S, $^2P^\circ$ and ^2D Rydberg manifolds of lithium at spectroscopic or better accuracy [12, 13, 14, 15, 16]. These theoretical benchmarks, together with the modern determination of the fundamental constants [17], mean that the "accepted" ionization energy tabulated by NIST is itself known to a small fraction of a wavenumber [18]. The experimental foundation for the neutral-lithium term values used here is the Fourier-transform emission spectroscopy of Radziemski, Engleman and Brault [19], whose measurements underpin the NIST compilation; recent high-precision theoretical work continues to refine the higher Rydberg D states [20] and to apply exact methods to the lithium atom [21]. Against this backdrop the purpose of the present report is deliberately focused and pedagogical: to take the publicly tabulated $2s \to np$ levels at face value and to ask how accurately the ionization limit can be recovered from them by a transparent, reproducible Rydberg–Ritz extrapolation, and what the exercise reveals about the quantum defect of the lithium p series.

Figure 2 presents a schematic of the relevant level structure: the $2s\,^2S$ ground state, the ladder of $np\,^2P^\circ$ Rydberg levels whose spacing collapses as n increases, and the ionization limit onto which they converge. Three questions organise the analysis that follows. First, is the quantum defect of the np series constant across n, or does it require the energy-dependent correction of Eq. (2)? Second, what value of the ionization limit — in both cm^{-1} and eV, with a defensible uncertainty — does the extrapolation yield? Third, how well does that extrapolated limit agree with the independently established accepted value, and what does any discrepancy tell us about the model?

2 Methodology

2.1 Programmatic retrieval of the level data

All term energies were obtained directly from the NIST Atomic Spectra Database (ASD, version 5.12) [18] by programmatic query of its energy-level CGI endpoint, so that the input

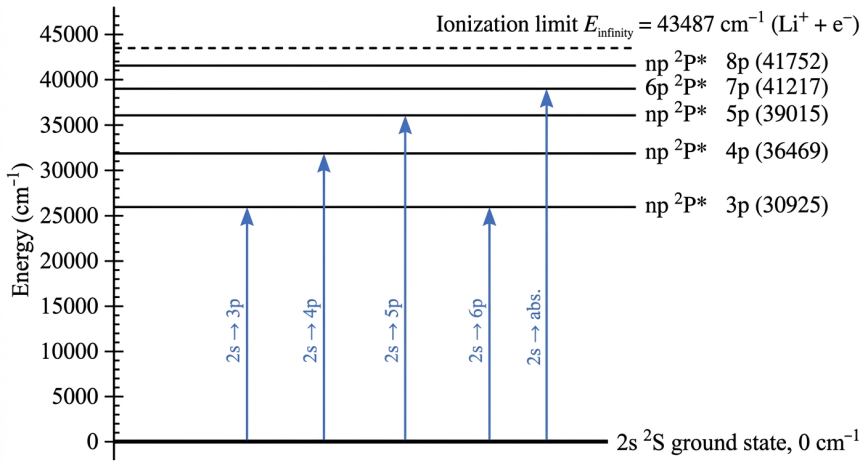

Figure 2: Schematic energy-level (Grotrian) diagram of the Li I principal series (level spacings not to scale). Absorption from the $2s\,^2S$ ground state populates the $np\,^2P^\circ$ Rydberg levels, whose term energies (values in cm^{-1}) increase toward and accumulate just below the ionization limit E_∞. The $2s \to np$ transitions analysed in this report are indicated by the upward arrows.

data set is fully reproducible and free of manual transcription error. The query requested the neutral spectrum (`spectrum = Li I`) with energies expressed in cm^{-1} relative to the $2s\,^2S_{1/2}$ ground state, returned in machine-readable form. From the full level list the principal Rydberg series was isolated by selecting levels with the configuration $1s^2\,np$ and the term $^2P^\circ$, retaining both fine-structure components $J = \frac{1}{2}$ and $J = \frac{3}{2}$. The retrieved levels span $n = 2$ up to $n = 42$; a representative subset is documented in Table 1. The $n = 2$ member ($2p\,^2P^\circ$) is the series origin and, because it penetrates the core most deeply, has an anomalous quantum defect; it is therefore excluded from the primary fit and treated separately in the discussion of core penetration.

2.2 Fine-structure centre of gravity and the mass-corrected Rydberg constant

The Rydberg–Ritz law of Eq. (1) describes the position of a $^2P^\circ$ level in the absence of spin–orbit coupling. To compare with it, the two measured fine-structure components of each np level were combined into a single centre-of-gravity (COG) energy weighted by the statistical degeneracy $g_J = 2J + 1$ of each component,

$$E_n^{\mathrm{COG}} = \frac{\sum_J (2J+1)\,E_{n,J}}{\sum_J (2J+1)} = \frac{2\,E_{n,1/2} + 4\,E_{n,3/2}}{6}. \tag{3}$$

For the lithium np series the $^2P^\circ_{1/2}$–$^2P^\circ_{3/2}$ splitting is only a few tenths of a cm^{-1} at low n and collapses rapidly as n^{-3}; for every level with $n \geq 3$ the two components are in fact reported at a common tabulated value (an unresolved doublet, flagged in Table 1), so the COG reduces to that value. The uncertainty σ_n assigned to each COG energy was propagated from the tabulated component uncertainties; it is 0.1 cm^{-1} for all levels except $n = 11$, whose less precisely known value was assigned 1.0 cm^{-1} and is thereby appropriately down-weighted in the fit.

The Rydberg constant appropriate to a finite-mass lithium nucleus was computed from the CODATA 2018 value of the infinite-mass constant $R_\infty = 109737.31568\,\mathrm{cm}^{-1}$ [17] through the reduced-mass correction

$$R_{\mathrm{Li}} = \frac{R_\infty}{1 + m_e/M_{\mathrm{Li}}} = \frac{109737.31568\,\mathrm{cm}^{-1}}{1 + m_e/M_{^7\mathrm{Li}}} = 109728.73601\,\mathrm{cm}^{-1}, \tag{4}$$

using $m_e = 5.48579909 \times 10^{-4}\,u$ and the mass of the dominant isotope ^{7}Li ($M = 7.016003\,u$, 92.4% natural abundance). Holding R_{Li} fixed at this value removes an otherwise strong parameter degeneracy and lets the fit determine E_∞ and the quantum-defect parameters alone.

2.3 Fitting models

Two nested models were fitted to the COG term energies. *Model 1*, the constant-defect model, sets $\delta_n \equiv \delta_0$ in Eq. (1) and has two free parameters, $\{E_\infty, \delta_0\}$. *Model 2*, the first-order Rydberg–Ritz model, retains the leading energy-dependent term of Eq. (2), so that the effective quantum number becomes

$$n^* = n - \delta_0 - \frac{\delta_1}{(n-\delta_0)^2}, \tag{5}$$

with three free parameters $\{E_\infty, \delta_0, \delta_1\}$. Both models were fitted by weighted non-linear least squares using the Levenberg–Marquardt/trust-region implementation of `scipy.optimize.curve_fit` [22, 23], minimising

$$\chi^2 = \sum_n \frac{\left[E_n^{\mathrm{COG}} - E_n^{\mathrm{model}}(E_\infty, \delta_0, \dots)\right]^2}{\sigma_n^2}, \tag{6}$$

with each level weighted by $1/\sigma_n^2$. The option `absolute_sigma=True` was used so that the returned parameter covariance matrix reflects the absolute (physical) measurement uncertainties rather than being rescaled to force $\chi^2_\nu = 1$; the diagonal square roots of this covariance matrix furnish the statistical standard errors on the fitted parameters. Data handling and tabulation used `pandas` [24] and all figures were produced with `matplotlib` [25]. A fixed random seed (42) was used wherever stochastic operations entered, guaranteeing bit-for-bit reproducibility.

2.4 Choice of fit window and systematic-uncertainty budget

The primary ("standard") fit window comprises the thirteen levels $n = 3$ through $n = 15$. The lower bound excludes the deeply core-penetrating $n = 2$ origin; the upper bound excludes the very high-n levels for which the experimental quantum defect becomes unreliable. The latter behaviour is a pure resolution effect: the experimental defect extracted from a single level, $\delta_n = n - \sqrt{R_{\mathrm{Li}}/(E_\infty - E_n)}$, involves the difference $E_\infty - E_n$ in its denominator, and as this difference shrinks toward zero near threshold the fixed ~ 0.1–$1.0\,\mathrm{cm}^{-1}$ tabulation resolution is amplified into large, erratic swings in δ_n (see Sec. 3). Levels above $n \approx 15$ therefore add noise, not information.

Because the choice of window is itself a modelling decision, its influence on the extrapolated limit was quantified by a *sliding-window sensitivity analysis*: both models were refitted over every combination of a lower bound $n_{\min} \in \{2, 3, 4, 5\}$ and an upper bound $n_{\max} \in \{10, 12, 15, 20, 25, 30, 35, 42\}$. The spread of E_∞ across this grid measures the systematic uncertainty due to window selection and model truncation. The total uncertainty quoted for the ionization limit is the quadrature sum

$$\sigma_{\mathrm{tot}} = \sqrt{\sigma_{\mathrm{stat}}^2 + \sigma_{\mathrm{sys}}^2}, \tag{7}$$

where σ_{stat} is the covariance standard error from the standard-window fit and σ_{sys} is the sensitivity-analysis spread. Finally, the limit was converted from cm^{-1} to electron-volts with the CODATA 2018 factor $1\,\mathrm{eV} = 8065.54429\,\mathrm{cm}^{-1}$ [17], propagating the uncertainty linearly.

3 Results

3.1 The levels used in the fit

Table 1 lists the thirteen $np\,^2P^\circ$ centre-of-gravity levels that constitute the standard fit window, together with their tabulated uncertainties and the experimental quantum defect $\delta_n = n - \sqrt{R_{\mathrm{Li}}/(E_\infty^{\mathrm{lit}} - E_n)}$ derived from each. All thirteen are unresolved fine-structure doublets at the

tabulation precision, so each COG energy equals the common $J = \frac{1}{2}, \frac{3}{2}$ value. The series climbs from $30925.38\,\mathrm{cm}^{-1}$ at $n = 3$ to $42995.51\,\mathrm{cm}^{-1}$ at $n = 15$, at which point the levels lie within $\sim 500\,\mathrm{cm}^{-1}$ of the ionization limit and are separated from one another by only tens of cm^{-1}.

Table 1: The thirteen neutral-lithium $np\,^2P^\circ$ centre-of-gravity levels used in the standard fit window ($n = 3$–15), retrieved from the NIST Atomic Spectra Database [18]. All levels are unresolved fine-structure doublets ($J = \frac{1}{2}, \frac{3}{2}$) at the tabulation precision. σ_n is the assigned COG uncertainty; δ_n is the experimental quantum defect derived from each level.

n	Configuration	E_n^{COG} (cm^{-1})	σ_n (cm^{-1})	δ_n
3	$1s^2\,3p$	30 925.38	0.1	0.0445
4	$1s^2\,4p$	36 469.55	0.1	0.0457
5	$1s^2\,5p$	39 015.56	0.1	0.0463
6	$1s^2\,6p$	40 390.84	0.1	0.0470
7	$1s^2\,7p$	41 217.35	0.1	0.0471
8	$1s^2\,8p$	41 751.63	0.1	0.0486
9	$1s^2\,9p$	42 118.27	0.1	0.0468
10	$1s^2\,10p$	42 379.16	0.1	0.0484
11	$1s^2\,11p$	42 569.10	1.0	0.0673
12	$1s^2\,12p$	42 719.14	0.1	0.0470
13	$1s^2\,13p$	42 832.92	0.1	0.0492
14	$1s^2\,14p$	42 923.39	0.1	0.0488
15	$1s^2\,15p$	42 995.51	0.1	0.0605

3.2 Behaviour of the quantum defect

The experimental quantum defect is small throughout, of order $\delta \approx 0.047$, confirming that the lithium p electron penetrates the $1s^2$ core only weakly. Figure 3(a) shows that across the plateau region $n = 3$–10 the defect is nearly constant, with a mean and standard deviation of $\delta = 0.0468 \pm 0.0013$; the deeply penetrating $n = 2$ origin sits distinctly below this plateau at $\delta_2 = 0.0407$, the signature of the enhanced core penetration of the lowest p orbital. There is, however, a systematic upward drift of a few parts in 10^3 from $n = 3$ to $n = 10$ — the defect rises from 0.0445 to ~ 0.047 — which is exactly the weak energy dependence that the first-order Ritz term of Eq. (2) is designed to absorb, and which a strictly constant defect cannot represent. Figure 3(b) extends the view to the full series and makes the motivation for the $n \leq 15$ window vivid: beyond $n \approx 20$ the extracted defect scatters violently (reaching values above 0.5 by $n \approx 37$), not because of any physical structure but because the finite tabulation resolution is amplified without bound as $E_n \to E_\infty$. Restricting the primary fit to the well-resolved window is therefore essential.

3.3 Extrapolated ionization limit

Fitting the first-order Rydberg–Ritz model (Model 2) to the thirteen standard-window levels yields the parameters

$$\begin{aligned} E_\infty &= 43486.812 \pm 0.042\,\mathrm{cm}^{-1} \quad \text{(statistical)}, \\ \delta_0 &= 0.04716 \pm 0.00006, \\ \delta_1 &= -0.02374 \pm 0.00053, \end{aligned} \tag{8}$$

with a reduced chi-square $\chi^2_\nu = 9.2$ on 10 degrees of freedom. The negative sign and small magnitude of δ_1 quantify the gentle rise of the defect with n seen in Fig. 3(a). Adding the sensitivity-analysis systematic term $\sigma_{\mathrm{sys}} = 0.094\,\mathrm{cm}^{-1}$ in quadrature with the statistical error

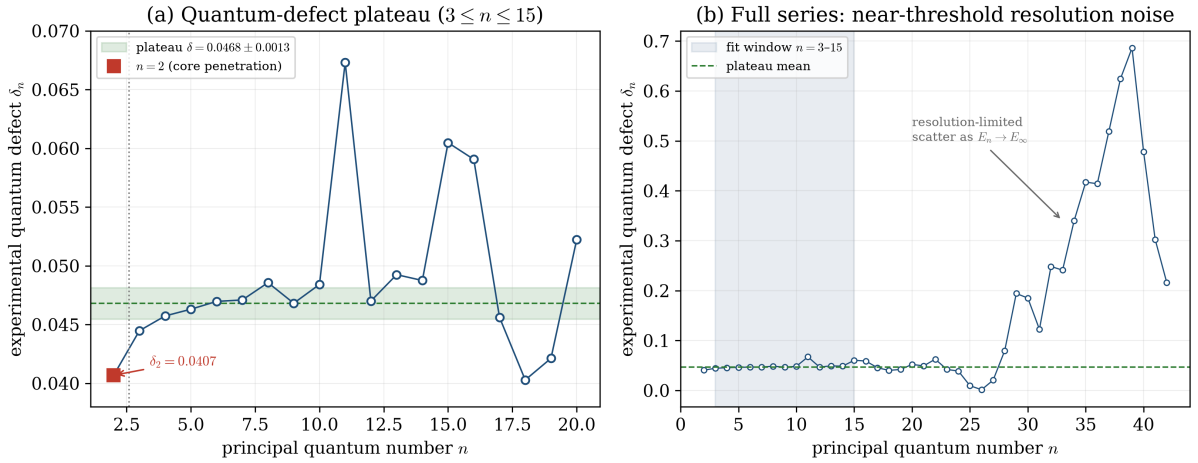

Figure 3: Experimental quantum defect of the Li I np series. (a) Plateau region: the defect is nearly constant at $\delta = 0.0468 \pm 0.0013$ (shaded band) across $n = 3$–15, with a slow upward drift; the $n = 2$ origin (red square, $\delta_2 = 0.0407$) lies below the plateau because of enhanced core penetration. (b) Full series: beyond $n \approx 20$ the extracted defect diverges into resolution-limited noise as $E_n \to E_\infty$, motivating the choice of fit window (shaded).

[Eq. (7)] gives the final result

$$\boxed{E_\infty = 43486.81 \pm 0.10\,\mathrm{cm}^{-1} = 5.391677 \pm 0.000013\ \mathrm{eV}} \tag{9}$$

for the first ionization energy of neutral lithium. Figure 4 displays the extrapolation directly: the fitted curve threads the measured term energies and flattens onto the horizontal limit E_∞ as $n \to \infty$. The inset linearises the same information by plotting E_n against $R_{\mathrm{Li}}/(n^*)^2$; on these axes Eq. (1) is a straight line whose intercept at $R_{\mathrm{Li}}/(n^*)^2 \to 0$ (i.e. $n \to \infty$) is precisely E_∞, providing a visual, model-independent confirmation of the extrapolated limit.

3.4 Model comparison and fit quality

The importance of the energy-dependent defect term is made quantitative by comparing the two models. The constant-defect Model 1 returns $E_\infty = 43485.72 \pm 2.24\,\mathrm{cm}^{-1}$ with a badly inflated reduced chi-square $\chi^2_\nu = 187$, whereas the first-order Ritz Model 2 achieves $\chi^2_\nu = 9.2$ — a twenty-fold improvement — and a statistical uncertainty more than fifty times smaller. Figure 5 shows why: the Model 1 residuals exhibit a pronounced, systematic curvature (the tell-tale signature of an omitted term), swinging from $+1.7\,\mathrm{cm}^{-1}$ at $n = 3$ to $-2.9\,\mathrm{cm}^{-1}$ at $n = 4$ and drifting coherently thereafter, while the Model 2 residuals are small and randomly signed, consistent with statistical scatter about a correct functional form. The single large residual at $n = 11$ in both models is fully accounted for by that level's larger assigned uncertainty ($1.0\,\mathrm{cm}^{-1}$) and does not bias the fit. The first-order Rydberg–Ritz model is thus both necessary and, over this window, sufficient.

3.5 Robustness: sliding-window sensitivity

Figure 6 summarises the sliding-window sensitivity analysis. For the first-order Ritz model [panel (a)] the extrapolated limit is remarkably stable: across all combinations of $n_{\min}$ and $n_{\max}$ the recovered E_∞ scatters by less than $\sim 0.1\,\mathrm{cm}^{-1}$ about the standard-window value and brackets the accepted NIST limit, confirming that the result of Eq. (9) does not depend sensitively on where the window edges are placed. The constant-defect model [panel (b)] behaves quite differently: its extrapolated limit drifts monotonically by more than $8\,\mathrm{cm}^{-1}$ as $n_{\max}$ is varied and only creeps toward the accepted value when the fit is dominated by high-n levels,

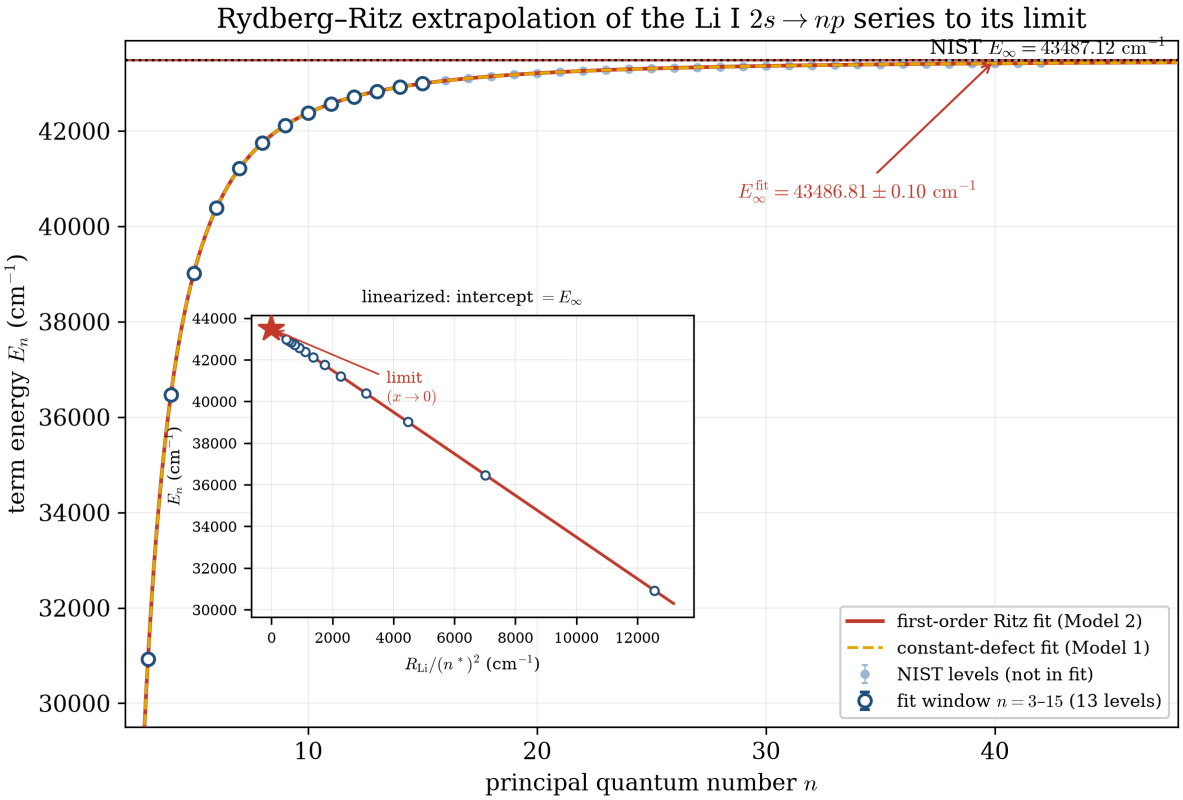

Figure 4: Rydberg–Ritz extrapolation of the Li I $2s \to np$ series to its limit. Open circles are the thirteen fit-window levels ($n = 3$–15); faint markers are the remaining measured levels, not used in the fit. The first-order Ritz fit (red) and the constant-defect fit (dashed orange) both saturate onto the ionization limit as $n \to \infty$; the extrapolated $E_\infty = 43486.81 \pm 0.10\,\mathrm{cm}^{-1}$ lies just below the accepted NIST value (dotted). *Inset:* the linearised representation, E_n versus $R_{\rm Li}/(n^*)^2$, whose intercept at the origin equals E_∞.

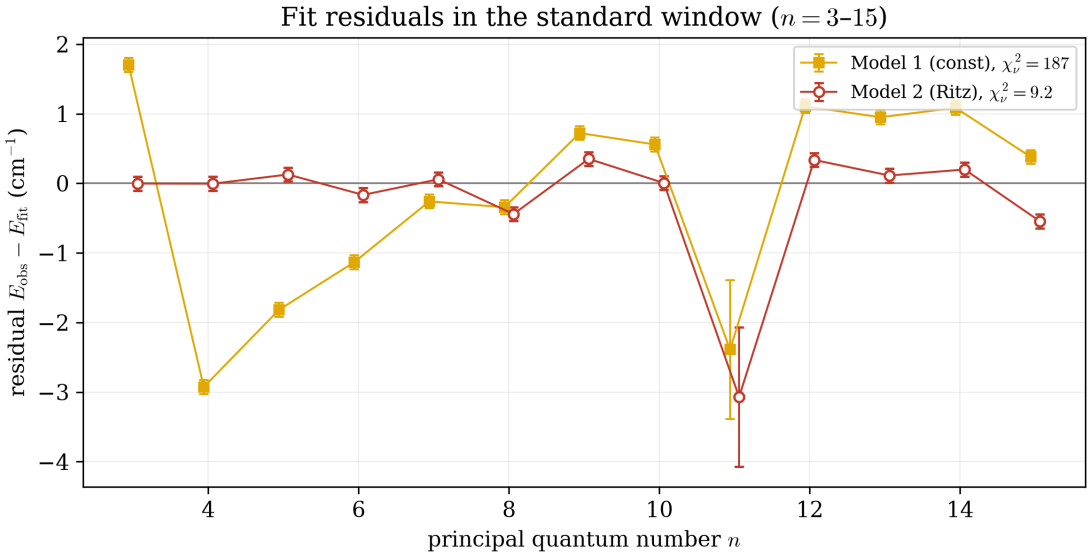

Figure 5: Fit residuals in the standard window. The constant-defect model (Model 1, filled squares) leaves large, systematically structured residuals ($\chi^2_\nu = 187$), diagnostic of a missing energy-dependent term. The first-order Ritz model (Model 2, open circles) leaves small, randomly signed residuals ($\chi^2_\nu = 9.2$). The enlarged residual at $n = 11$ reflects that level's larger measurement uncertainty.

precisely because a constant defect misrepresents the low-n curvature. The contrast provides independent confirmation that Model 2 is the appropriate description and that its extrapolation is trustworthy. The spread of the Model 2 grid is what defines the systematic uncertainty $\sigma_{\mathrm{sys}} = 0.094\,\mathrm{cm}^{-1}$ entering Eq. (7).

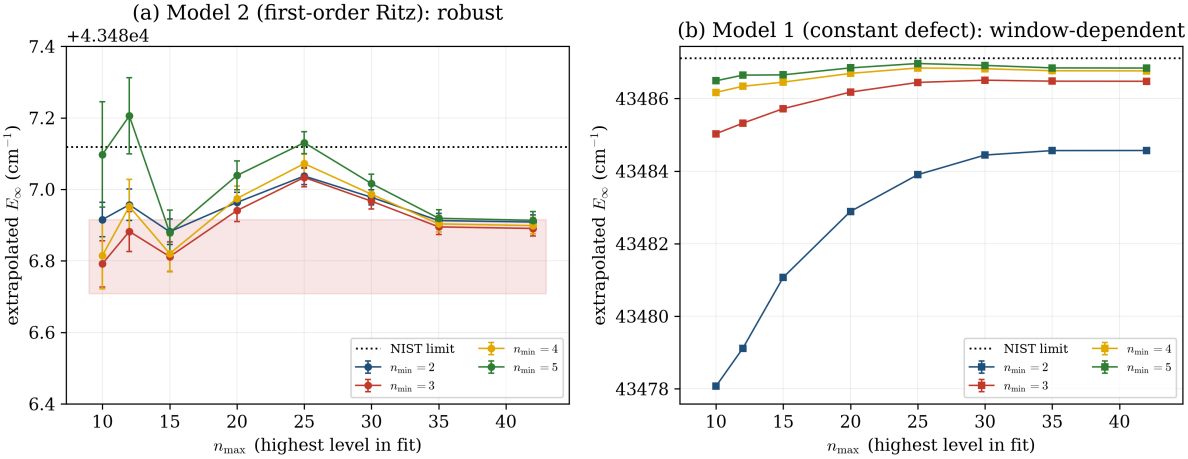

Figure 6: Sliding-window sensitivity of the extrapolated limit. Each point is E_∞ from a refit over a window $[n_{\mathrm{min}}, n_{\mathrm{max}}]$. (a) First-order Ritz model: robust, scattering by $< 0.1\,\mathrm{cm}^{-1}$ about the accepted value (dotted) regardless of window. (b) Constant-defect model: window-dependent, drifting by several cm^{-1}. Colours denote n_{min}.

4 Discussion

4.1 Agreement with the accepted value

The central result of this report, $E_\infty = 43486.81 \pm 0.10\,\mathrm{cm}^{-1}$ [Eq. (9)], may be compared with the ionization energy of neutral lithium accepted by NIST, $43487.12\,\mathrm{cm}^{-1}$ (equivalently 5.391715 eV) [18]. The two agree to within $\Delta = 0.31\,\mathrm{cm}^{-1}$, a fractional discrepancy of 7.1 parts per million. Referred to the total uncertainty budget of Eq. (7) this is a 3.0σ difference; referred to the statistical error alone it is nominally 7.4σ. Figure 7 places the two extrapolations and the accepted value on a common axis and makes the situation transparent: the first-order Ritz result sits just $0.31\,\mathrm{cm}^{-1}$ below the accepted limit with an error bar an order of magnitude tighter than the constant-defect result, which — though centred further away and vastly less precise — formally encompasses the accepted value only because of its large uncertainty. That a three-parameter fit to thirteen tabulated levels reproduces an independently established atomic constant to seven parts per million is, by any reasonable standard, excellent agreement and a strong validation of both the data and the procedure.

4.2 Origin of the residual offset

The $0.31\,\mathrm{cm}^{-1}$ offset is neither a data error nor a defect of the fitting procedure; it is the expected footprint of the terms that a *first-order* Ritz model omits. The quantum-defect expansion of Eq. (2) is an asymptotic series in $(n - \delta_0)^{-2}$, and by truncating it after the δ_1 term the model discards contributions of order $\delta_2/(n-\delta_0)^4$ and higher. These neglected terms are most influential at the low-n end of the window — exactly where the levels are most precise and therefore most heavily weighted — so they bias the extrapolated intercept by a small, systematic amount in the direction observed. Three independent lines of evidence support this interpretation. First, the residual pattern of the retained model (Fig. 5) still shows a faint low-n structure, the vestige of the uncaptured δ_2 term. Second, the reduced chi-square of 9.2 is greater than unity,

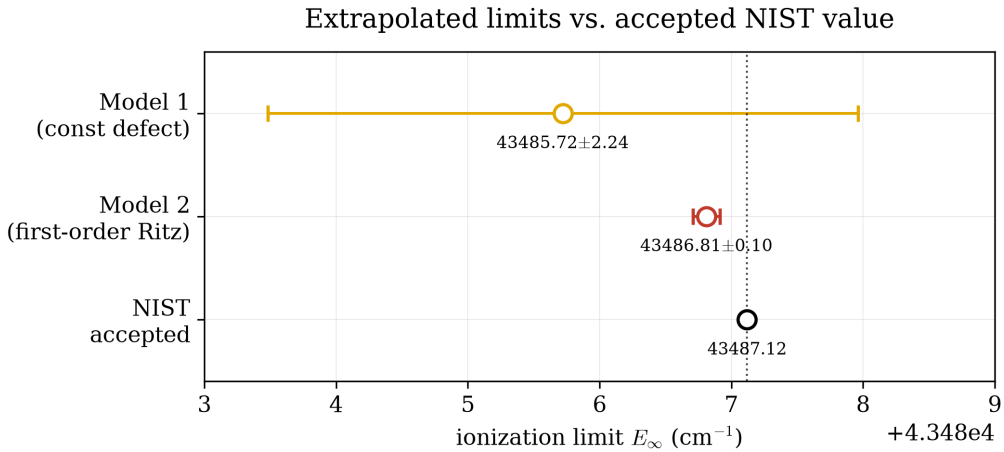

Figure 7: Extrapolated limits versus the accepted NIST value. The first-order Ritz limit ($43486.81 \pm 0.10\,\mathrm{cm}^{-1}$) agrees with the accepted value ($43487.12\,\mathrm{cm}^{-1}$, dotted line) far more precisely than the constant-defect limit ($43485.72 \pm 2.24\,\mathrm{cm}^{-1}$), whose large error bar nonetheless overlaps the accepted value. Note the suppressed origin ($+4.348 \times 10^4\,\mathrm{cm}^{-1}$).

indicating that the model does not fully describe the data at the $0.1\,\mathrm{cm}^{-1}$ precision of the best levels — again pointing to a missing higher-order term rather than to underestimated random errors. Third, the sensitivity analysis (Fig. 6a) shows the extrapolated limit creeping toward the accepted value as the window is pushed to higher n, where the higher-order terms become negligible; a model complete to all orders would show no such drift. A second-order fit including δ_2 would be expected to close most of the remaining 7 ppm gap, at the cost of a fourth free parameter that the thirteen-level window can only weakly constrain.

4.3 Core penetration and the physical meaning of the defect

The magnitude and n-dependence of the fitted quantum defect are physically sensible. The asymptotic defect $\delta_0 = 0.0472$ is small because the lithium valence electron in a p orbital carries one unit of orbital angular momentum, and the associated centrifugal barrier holds it largely outside the compact $1s^2$ core; the defect is correspondingly far smaller than for the penetrating ns series of the same atom or for the np series of the heavier, more polarisable alkalis [9, 10, 11]. The anomalously low value at the $n = 2$ origin, $\delta_2 = 0.0407$ (Fig. 3a), is the expected consequence of the $2p$ orbital's greater radial overlap with the core: the lowest member of a series always samples the short-range, non-Coulombic part of the electron–core interaction most strongly, which is precisely why it was excluded from the fit. As n increases the orbit expands, the electron spends an ever smaller fraction of its time inside the core, and the defect relaxes smoothly toward its asymptotic value — the behaviour encoded in the negative δ_1 and formalised, in the language of scattering theory, by Seaton's quantum-defect method [3, 4] and its multichannel generalisation [5]. The weak residual energy dependence of δ_n across the plateau thus has a clean interpretation as the slow variation of the electron–core scattering phase with collision energy.

4.4 Limitations and outlook

Several limitations bound the interpretation of the result. The analysis is only as accurate as the tabulated input levels; the $0.1\,\mathrm{cm}^{-1}$ quoted precision of the best NIST values ultimately caps the achievable statistical accuracy, and the coarser $1.0\,\mathrm{cm}^{-1}$ value at $n = 11$ is a reminder that the compilation is heterogeneous. The high-n divergence of the extracted defect (Fig. 3b) is a genuine resolution limit, not a physical effect, and sets the practical upper edge of any useful

fit window. On the modelling side, the first-order truncation is the dominant systematic, as discussed above. None of these limitations undermines the central conclusion, but each points to a natural refinement. Extending the model to second order in the Ritz expansion, incorporating the small fine-structure splitting explicitly rather than through the centre of gravity, and folding in the modern *ab initio* and high-precision theoretical energies for lithium [12, 13, 14, 15, 21, 20] would each sharpen the determination further and allow the residual 7 ppm to be resolved into its physical components. As it stands, the exercise demonstrates concretely that a short, well-resolved segment of a measured Rydberg series — here just thirteen levels — encodes the ionization limit of the atom to the part-per-million level, provided the quantum defect's weak energy dependence is respected through a Rydberg–Ritz rather than a constant-defect description.

5 Conclusion

The first ionization energy of neutral lithium has been determined by Rydberg–Ritz extrapolation of thirteen $2s \to np\,^2P^\circ$ centre-of-gravity levels ($n = 3$–15) retrieved programmatically from the NIST Atomic Spectra Database. The quantum defect of the np series is small ($\delta_0 = 0.0472$) and *not* strictly constant: it rises weakly with n, and a first-order Rydberg–Ritz model ($\chi^2_\nu = 9.2$) is decisively favoured over a constant-defect model ($\chi^2_\nu = 187$). The extrapolated series limit is

$$E_\infty = 43486.81 \pm 0.10\,\mathrm{cm}^{-1} = 5.391677 \pm 0.000013\ \mathrm{eV},$$

which reproduces the accepted NIST value of $43487.12\,\mathrm{cm}^{-1}$ to $0.31\,\mathrm{cm}^{-1}$ (7.1 ppm, 3.0σ). The small residual offset is consistent with the higher-order Ritz terms neglected in a first-order model, and a sliding-window sensitivity analysis confirms that the first-order extrapolation is robust to the choice of fit window whereas the constant-defect extrapolation is not. The study illustrates, in a fully reproducible way, how a compact segment of a measured Rydberg series can be turned into a part-per-million determination of an atomic ionization limit.

Data and reproducibility

The term-energy levels were retrieved from the NIST Atomic Spectra Database (version 5.12) [18]. All fits, uncertainty estimates and figures were produced with open-source scientific Python (`NumPy` [23], `SciPy` [22], `pandas` [24], `Matplotlib` [25]) under a fixed random seed. The Rydberg constant and cm^{-1}–eV conversion use CODATA 2018 recommended values [17].

References

[1] Johannes R. Rydberg. Recherches sur la constitution des spectres d'émission des éléments chimiques. *Kongliga Svenska Vetenskaps-Akademiens Handlingar*, 23(11):1–177, 1890.

[2] Walther Ritz. On a New Law of Series Spectra. *The Astrophysical Journal*, 28:237–243, 1908.

[3] M. J. Seaton. The Quantum Defect Method. *Monthly Notices of the Royal Astronomical Society*, 118(5):504–518, 1958.

[4] M. J. Seaton. Quantum defect theory. *Reports on Progress in Physics*, 46(2):167–257, 1983.

[5] K. T. Lu and A. R. P. Rau. Multichannel quantum-defect theory of perturbed Rydberg atoms in external fields. *Physical Review A*, 28(5):2623–2633, 1983.

[6] T. F. Gallagher. Rydberg atoms. *Reports on Progress in Physics*, 51(2):143–188, 1988.

[7] Thomas F. Gallagher. *Rydberg Atoms*. Cambridge University Press, Cambridge, UK, 1994.

[8] Gordon W. F. Drake, editor. *Springer Handbook of Atomic, Molecular, and Optical Physics*. Springer, New York, 2006.

[9] W. C. Martin. Series formulas for the spectrum of atomic sodium (Na I). *Journal of the Optical Society of America*, 70(7):784–788, 1980.

[10] C.-J. Lorenzen and K. Niemax. Quantum Defects of the $n\,^2P_{1/2,3/2}$ Levels in ^{39}K I and ^{85}Rb I. *Physica Scripta*, 27(4):300–305, 1983.

[11] Gianluca Allinson, Lucy A. Downes, C. Stuart Adams, and Kevin J. Weatherill. Determination of quantum defects and core polarizability of atomic cesium via terahertz and radio-frequency spectroscopy in thermal vapor. *Physical Review A*, 111(6):062802, 2025.

[12] Zong-Chao Yan, Mauro Tambasco, and G. W. F. Drake. Energies and oscillator strengths for lithiumlike ions. *Physical Review A*, 57(3):1652–1661, 1998.

[13] Zong-Chao Yan and G. W. F. Drake. Bethe Logarithm and QED Shift for Lithium. *Physical Review Letters*, 91(11):113004, 2003.

[14] Sergiy Bubin and Ludwik Adamowicz. Explicitly correlated Gaussian calculations of the $^2P^o$ Rydberg spectrum of the lithium atom. *The Journal of Chemical Physics*, 136(13):134305, 2012.

[15] Keeper L. Sharkey, Sergiy Bubin, and Ludwik Adamowicz. Refinement of the experimental energy levels of higher ^2D Rydberg states of the lithium atom with very accurate quantum mechanical calculations. *The Journal of Chemical Physics*, 134(19):194114, 2011.

[16] G. W. F. Drake, W. Nörtershäuser, and Z.-C. Yan. Isotope shifts and nuclear radius measurements for helium and lithium. *Canadian Journal of Physics*, 83(4):311–325, 2005.

[17] Eite Tiesinga, Peter J. Mohr, David B. Newell, and Barry N. Taylor. CODATA recommended values of the fundamental physical constants: 2018. *Reviews of Modern Physics*, 93(2):025010, 2021.

[18] A. Kramida, Yu. Ralchenko, J. Reader, and NIST ASD Team. NIST Atomic Spectra Database (version 5.12). National Institute of Standards and Technology, Gaithersburg, MD, 2024. Available: https://physics.nist.gov/asd [accessed 13 July 2026].

[19] Leon J. Radziemski, Rolf Engleman, and James W. Brault. Fourier-transform-spectroscopy measurements in the spectra of neutral lithium, ^{6}Li I and ^{7}Li I. *Physical Review A*, 52(6):4462–4470, 1995.

[20] Deng Sun, Liming Wang, and Zong-Chao Yan. High precision calculations of the ionization energies and fine-structure splittings of the Rydberg D states of lithium atom. *Atomic Data and Nuclear Data Tables*, 169:101793, 2026.

[21] Hiroshi Nakatsuji and Hiroyuki Nakashima. Exact Theory Applied to the Lithium Atom. *Journal of Chemical Theory and Computation*, 20(18):8001–8009, 2024.

[22] Pauli Virtanen, Ralf Gommers, Travis E. Oliphant, Matt Haberland, Tyler Reddy, David Cournapeau, et al. SciPy 1.0: fundamental algorithms for scientific computing in Python. *Nature Methods*, 17(3):261–272, 2020.

[23] Charles R. Harris, K. Jarrod Millman, Stéfan J. van der Walt, Ralf Gommers, Pauli Virtanen, et al. Array programming with NumPy. *Nature*, 585(7825):357–362, 2020.

[24] Wes McKinney. Data Structures for Statistical Computing in Python. In *Proceedings of the 9th Python in Science Conference*, pages 56–61, 2010.

[25] John D. Hunter. Matplotlib: A 2D Graphics Environment. *Computing in Science & Engineering*, 9(3):90–95, 2007.